Fabrication of VO_2 thin film by rapid thermal annealing in oxygen atmosphere and its metal–insulator phase transition properties*

Liang Ji-Ran(梁继然)[a)†], Wu Mai-Jun(吴励君)[a)], Hu Ming(胡 明)[a)], Liu Jian(刘 剑)[b)], Zhu Nai-Wei(朱乃伟)[a)], Xia Xiao-Xu(夏晓旭)[a)], and Chen Hong-Da(陈弘达)[c)]

[a)] *School of Electronic Information and Engineering, Tianjin University, Tianjin* 300072, *China*

[b)] *State Key Laboratory for Super Lattices and Microstructures, Institute of Semiconductors, Chinese Academy of Sciences, Beijing* 100083, *China*

[c)] *State Key Laboratory of Integrated Optoelectronics, Institute of Semiconductors, Chinese Academy of Sciences, Beijing* 100083, *China*

(Received 5 November 2013; revised manuscript received 23 January 2014; published online 15 May 2014)

Vanadium dioxide thin films have been fabricated through sputtering vanadium thin films and rapid thermal annealing in oxygen. The microstructure and the metal–insulator transition properties of the vanadium dioxide thin films were investigated by X-ray diffraction, X-ray photoelectron spectroscopy, and a spectrometer. It is found that the preferred orientation of the vanadium dioxide changes from $(\bar{1}11)$ to (011) with increasing thickness of the vanadium thin film after rapid thermal annealing. The vanadium dioxide thin films exhibit an obvious metal–insulator transition with increasing temperature, and the phase transition temperature decreases as the film thickness increases. The transition shows hysteretic behaviors, and the hysteresis width decreases as the film thickness increases due to the higher concentration carriers resulted from the uncompleted lattice. The fabrication of vanadium dioxide thin films with higher concentration carriers will facilitate the nature study of the metal–insulator transition.

Keywords: vanadium dioxide, metal–insulator transition, rapid thermal annealing, hysteresis

PACS: 68.55.jd, 78.20.–e, 73.50.Lw **DOI:** 10.1088/1674-1056/23/7/076801

1. Introduction

Vanadium dioxide (VO_2) undergoes a first-order metal–insulator transition (MIT) at the critical temperature T_c = 68 °C.[1] The transition is accompanied by a structural change between a high-temperature tetragonal rutile structure and a low-temperature monoclinic rutile structure. The optical and electrical characters, such as transmittance, reflectivity, and conductivity, change distinctly.[2–5] Due to the repeatable and reversible phase transition properties, VO_2 is considered to be a promising candidate material for thermal excitation electronic and optical devices, such as heat detection devices, sensors, smart windows, optical switchers, and modulation devices in sub-micron wavelength.[6–10]

The fabrication of VO_2 thin films is important for their all kinds of applications. Many methods have been used to fabricate VO_2 thin films, such as chemical vapor deposition, reactive magnetron sputtering, sol–gel method, and pulsed laser deposition.[11–15] In this paper, we will show another method to fabricate VO_2 thin films, in which the films are prepared through rapid thermal annealing vanadium metal thin films in oxygen.

Rapid thermal annealing (RTA) is a semiconductor process used for the activation of dopants and the interfacial reaction of metal contacts. Now, this technology has been extended to the oxidation of transition metals. It has been used in the fabrication of the V_2O_5/p-Si rectifying junction, VO_2 thin films in air, and VO_x thin films.[16–18] It has been proved that RTA is an effective method to make V activated and oxidized.[18] However, there are few reports on the effects of the vanadium film thickness on the microstructure and the metal–insulator transition properties of the VO_2 thin films prepared by RTA.

In this paper, we deposited vanadium metal thin films with different thicknesses by magnetron sputtering, and then annealed them in oxygen atmosphere. We reported the influence of the vanadium thin film thickness on the microstructure and the electrical and optical transition properties.

2. Material fabrication and characterization methods

VO_2 thin films were prepared through the oxidation of vanadium thin films in oxygen using RTA. The vanadium thin films were deposited on c-type Al_2O_3 (0001) substrates by means of direct current facing target magnetron sputtering. The substrates were cleaned ultrasonically in ethanol, acetone, and deionized water followed by drying using a high pressure N_2 gas. The vanadium metal (99.99% purity) was sputtered in Ar atmosphere. The base pressure of the chamber was 2.4×10^{-4} Pa. The flux of Ar was 48 SCCM and controlled by a mass flow meter. The substrate was held at room temper-

*Project supported by the National Natural Science Foundation of China (Grant No. 61101055) and the Research Fund for the Doctoral Program of Higher Education, China (Grant No. 20100032120029).

†Corresponding author. E-mail: liang_jiran@tju.edu.cn

© 2014 Chinese Physical Society and IOP Publishing Ltd

ature, the sputtering power was 135 W, and the sputtering pressure was 0.5 Pa. In order to eliminate the contamination on the target surface, pre-sputtering of the vanadium target was performed before the vanadium thin film depositing. The thickness of the vanadium thin film was controlled by the sputtering time; the sputtering time was 10 min, 15 min, and 20 min, the thickness was 70 nm, 100 nm, and 120 nm, respectively. After the deposition, the films were annealed in an ultra pure oxygen ambient in a furnace (ALLWIN AG 610). According to other researcher's results,[19] the annealing temperature was set at 450 °C and the annealing time was 180 s. The flux of O_2 was 3 SCCM. The annealed vanadium thin films with sputtering time 10 min, 15 min, and 20 min are named S1, S2, and S3, respectively, for the convenience of presentation.

X-ray diffraction (XRD) (Rigaku, D/MAX2500V/PC) patterns using the Cu $K\alpha$ radiation ($\lambda = 0.15418$ nm) were examined to identify the crystalline phases of the vanadium oxide thin films. The composition and the valence of the annealed films were analyzed by X-ray photoelectron spectroscopy (XPS) (PHI1600). The optical transmittance spectra were obtained by a spectrometer in the wavelength range of 400–900 nm. In order to investigate the electrical properties, the sheet resistance was measured by using a four-point probe equipped with a heater.

3. Results and discussion

3.1. Crystal structure and composition

Figure 1 shows the XRD patterns of S1, S2, and S3. The S1 shows four diffraction peaks, and the peaks at $2\theta = 26.89°$ and $2\theta = 37.13°$ belong to VO_2 ($\bar{1}11$) and (200), respectively, according to JPCDS card No. 72-0514. The other two peaks at $2\theta = 17.83°$ and $2\theta = 45.58°$ belong to V_2O_5. As the thickness increases, S2 and S3, the intensities of the peaks of V_2O_5 decrease and disappear, however another V_2O_5 peak appears at 2θ = 20.53° (S3). From the XRD results, we can see that those three films are polycrystalline and have a mixed phase. It is interesting that the main orientation of VO_2 changes from ($\bar{1}11$) to (011). The change of the orientation shows that the distance between the crystal planes decreases. This may attribute to the insufficient oxygen in annealing for the increasing thickness under the same annealing conditions. The free energy of (011) is lower than that of ($\bar{1}11$), so the (011) orientation is preferred. This result may suggest that we can tune the orientation of monoclinic VO_2 by the thickness in RTA.

The detailed compositions of the samples were confirmed by XPS measurements as depicted in Fig. 2. Figure 2(a) shows the high-resolution spectrum of the V $2p_{3/2}$ core levels of S1, and the peak position is fitted by using a Shirley function with an XPS software. It is obvious that two main types of vanadium valences coexist in the film, namely, +4 valence with a binding energy of 516.6 eV and +5 valence with a binding energy of 517.7 eV. There is also an unobvious peak which results from another lower valence V ion. The concentrations of +4 and +5 V ions in the three films are plotted in Fig. 2(b). The concentrations of VO_2 in all films are near 60%, and that of V_2O_5 decreases as the thickness increases.

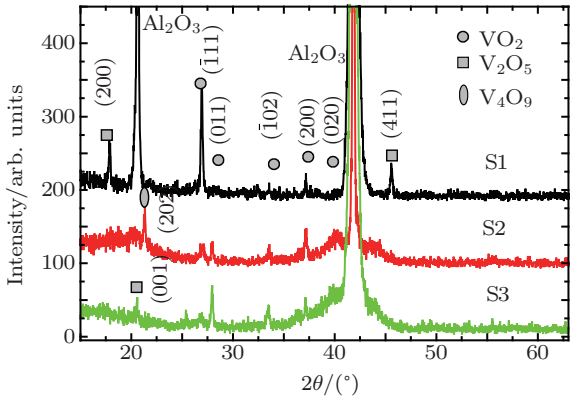
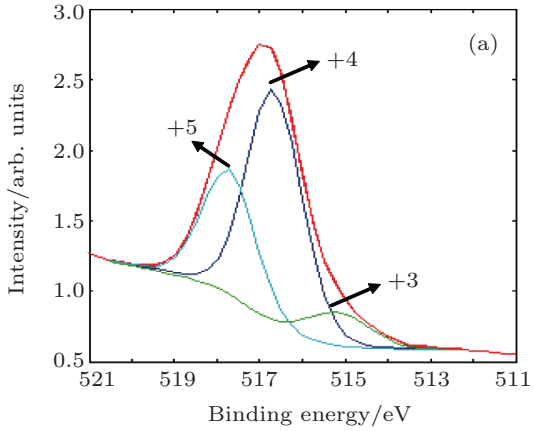


Fig. 1. (color online) The XRD patterns of the films.



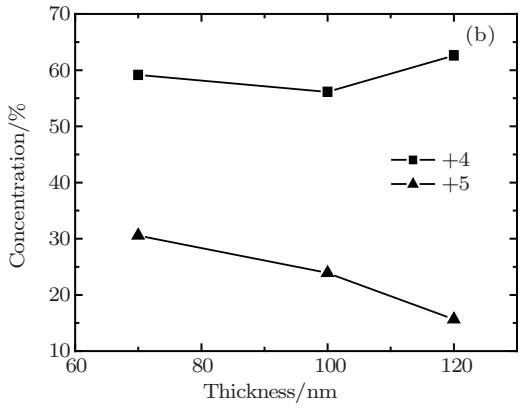


Fig. 2. (color online) (a) High-resolution XPS spectrum of the V $2p_{3/2}$ core levels of S1. (b) Concentrations of +5 and +4 V ions in the films.

The XRD and XPS results suggest that, under the same oxidization annealing condition, the degree of oxidation of vanadium declines as the thickness increasees, and it is easy to form (011) orientation VO_2 in the lower oxidation state.

3.2. Electrical and optical properties

Figure 3 presents the sheet resistance as a function of the heating temperature for the films. One can see clearly that the films show drops of resistance at near 50 °C, which is the typical property of crystalline VO_2. The sheet resistances of the films are very different, the sheet resistances R_s are 28 kΩ/□, 0.12 kΩ/□, and 0.06 kΩ/□ for S1, S2, and S3, respectively. The sheet resistance of S3 is close to that of a metal. However, all the films show the typical thermal activated conducting properties of a semiconductor near room temperature.

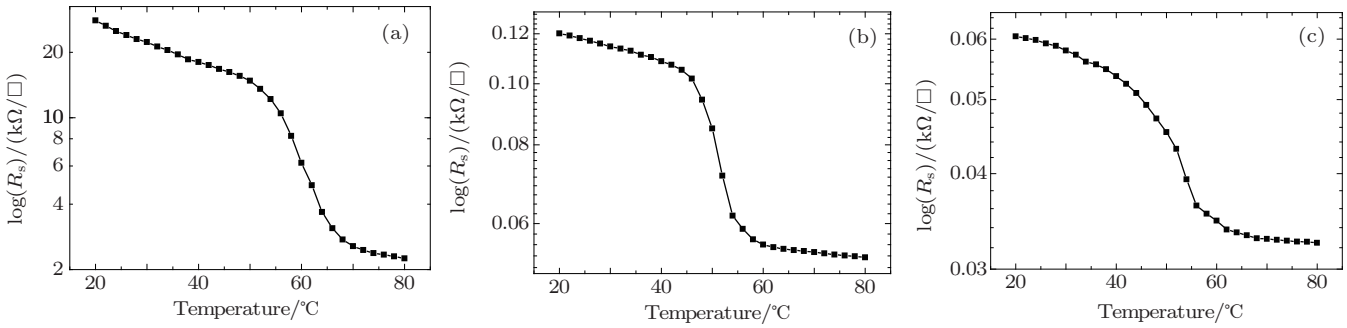


Fig. 3. The sheet resistance R_s versus heating temperature for (a) S1, (b) S2, and (c) S3.

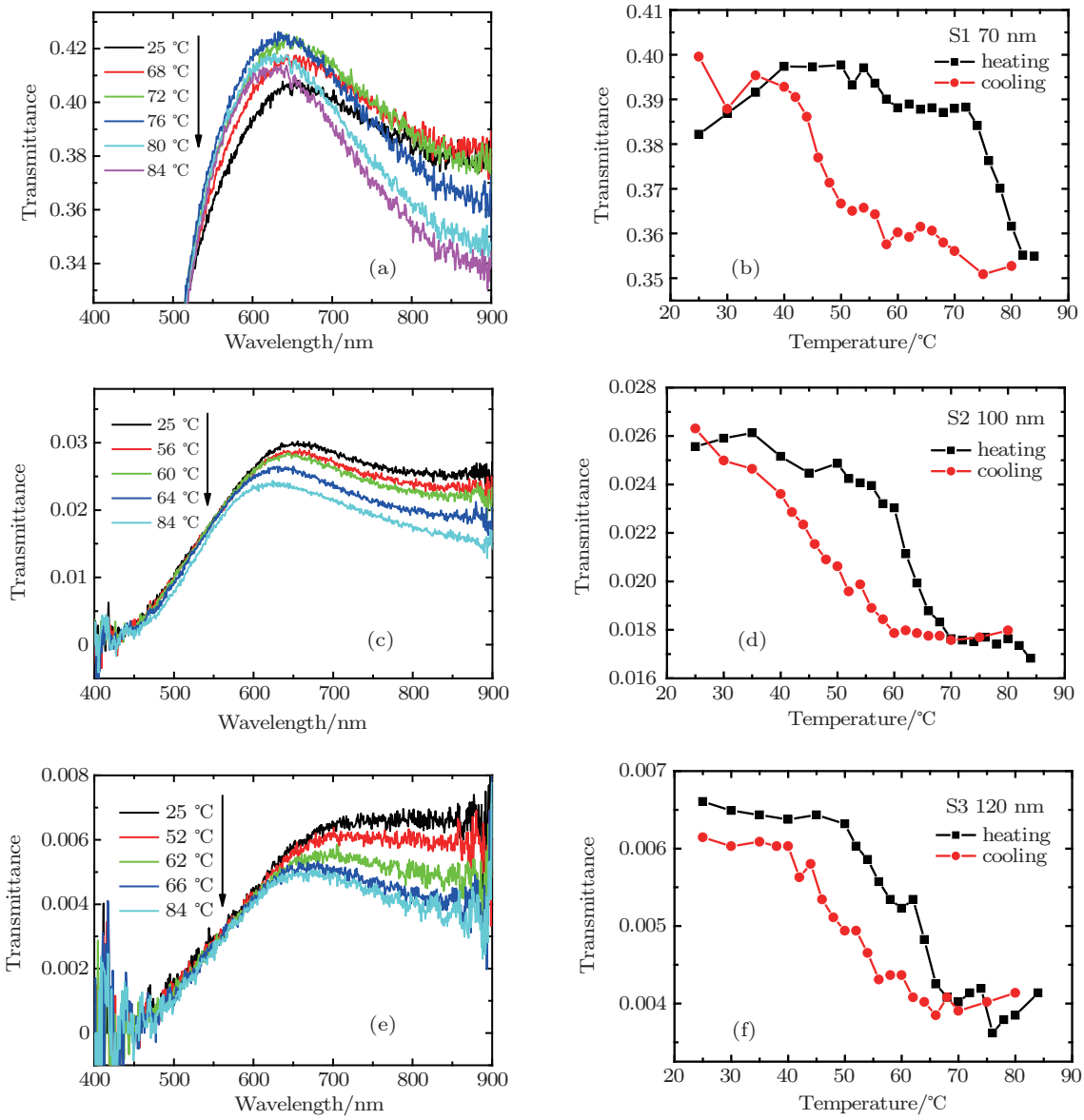


Fig. 4. (color online) Transmittance-wavelength plots at various temperatures and transmittance–temperature plots at $\lambda = 800$ nm: (a) and (b) S1, (c) and (d) S2, (e) and (f) S3.

According to the semiconductor theory, we can deduce the temperature coefficient of resistance (TCR) and the activation energy (ΔE) from the temperature dependence of the resistance qualitatively via the following relations:

$$R_s = R_{s0}\exp(\Delta E/kT), \tag{1}$$

$$R_s^{-1}(\mathrm{d}R_s/\mathrm{d}T) = \mathrm{TCR} = -\Delta E/kT^2, \tag{2}$$

where k is the Boltzmann constant, and T is the absolute temperature. Near room temperature, we have $\mathrm{TCR}_{S1} = -2.2$ %/°C, $\mathrm{TCR}_{S2} = -0.85$ %/°C, $\mathrm{TCR}_{S3} = -0.65$ %/°C and $\Delta E_{S1} = 0.18$ eV, $\Delta E_{S2} = 0.069$ eV, $\Delta E_{S3} = 0.052$ eV. For a crystalline semiconductor, ΔE is the energy interval from the bottom of the conduction band (E_c) to the Fermi level (E_F), namely, $\Delta E = E_c - E_F \approx (E_c - E_v)/2 = E_g/2$, where E_v is the valence-band top, and E_g is the band gap. We notice that ΔE decreases as the thickness increases after RTA in oxygen. However, ΔE is much lower than that of VO_2 single crystal.[20] This is due to the presence of defects or oxygen vacancies in the annealed films.

Figure 4 presents the optical properties of VO_2 thin films in the visual band. The room temperature transmittance of S1 is about 40%. As the thickness increases, the transmittance decreases, it is only 0.6% for S3. Figures 4(b), 4(d), and 4(f) show the temperature dependence of transmittance at a fixed wavelength of 800 nm. The three samples exhibit an obvious change with temperature increasing or decreasing, which is caused by the metal–insulator transition of VO_2.

These transitions show a hysteretic character. We compute the phase transition temperature T_T and the hysteretic width ΔH for those three films. Figure 5 shows the $\mathrm{d}T_r/\mathrm{d}T$–$T$ curves, which are fitted with Gaussian functions using the peak fitting module of Originpro 7.0 software. The centers of the Gaussian peaks are defined as the phase transition temperature T_T, and T_{TH} and T_{TC} represent the phase transition temperatures of heating and cooling branches, respectively. The ΔH is defined as the difference between T_{TH} and T_{TC}. The T_{TH} and ΔH of S1 are depicted in Fig. 5 according to the literature.[21] The hysteretic width ΔH is about 30 °C, and decreases as the thickness of the VO_2 thin film increases, and it is about 11 °C for S3, see Fig. 5(b). The phase transition temperature shows the same change trend as the hysteretic width.

The square resistance decreases sharply as the thickness of the vanadium thin film increases via the same RTA in oxygen. This means that there are more carriers in thicker films. From XRD and XPS results, the main compositions in the films are VO_2 and V_2O_5, and they are well crystallized. The concentration of lower valence V ions is low and can not result in such a low square resistance. So, from these results, we can conclude that the crystalline structure of the thicker film is uncompleted, and there are more O vacancies in the thicker film. The lower transmittance at room temperature is caused by the absorption of free carries in the thicker film.

We compare the transition temperatures calculated from the electronic properties and the optical properties. It is found that the transition temperature of the electronic transition is lower than that of the optical transition for the random transition process.[22]

The origin of the phase transition, whether is caused by the electron–electron correlation or the structure change, has been debated for a long time. It has been found that the transition occurs when the electron carriers in the insulator reach a critical density. The electron injection[23–25] has effects on the transition properties. And the uncompleted lattice structure resulted in large carriers can destabilize the semiconducting state and make the transition temperature lower and the hysteretic width narrower.

The higher concentration carries in VO_2 thin films destabilize the insulator state and change the transition properties. However the effect of the inter carriers on the transition is still unknown. The fabrication of VO_2 thin films with higher carriers will facilitate the studies of the inter carriers on the transition properties and the nature of the metal–insulator transition.

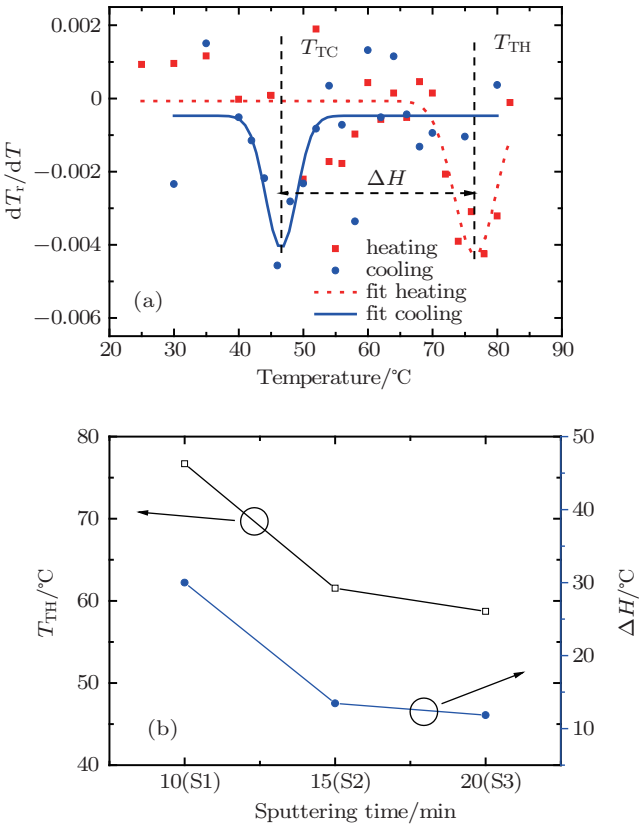


Fig. 5. (color online) (a) The $\mathrm{d}T_r/\mathrm{d}T$–$T$ curves of S1, (b) the phase transition temperature and the hysteresis width of three VO_2 films.

4. Conclusion

In conclusion, we have prepared monoclinic VO_2 thin films through RTA pure vanadium thin films in oxygen ambi-

ent, and studied the optical properties in the visual band across the phase transition. The lattice structure becomes uncompleted as the thick increases when annealed under the same RTA conditions. The VO_2 (011) orientation is preferred with a higher carrier density, and the carriers can decrease the phase transition temperature and the hysteretic width of the phase transition.

References

[1] Morin F J 1959 *Phys. Rev. Lett.* **3** 34
[2] Balu R and Ashrit P V 2008 *Appl. Phys. Lett.* **92** 21904
[3] Guinneton F, Sauques L, Valmalette J C, Cros F and Gavarri J R 2001 *J. Phys. Chem. Solids.* **62** 1229
[4] Wang X J, Liu Y Y, Li D H, Feng B H, He Z W and Qi Z 2013 *Chin. Phys. B* **22** 066803
[5] Zhang K L, Liu K, Wang F, Yin F H, Wei X Y and Zhao J S 2013 *Chin. Phys. B* **22** 097101
[6] Kiri P, Warwick M E A, Ridley I and Binions R 2011 *Thin Solid Films* **520** 1363
[7] Strelcov E, Lilach Y and Kolmakov A 2009 *Nano Lett.* **9** 2322
[8] Li G, Yuan N, Li J and Chen X 2006 *Sensor. Actuat. A Phys.* **126** 430
[9] Sweatlock L A and Diest K 2012 *Opt. Express* **20** 8700
[10] Liu Z Q, Chang S J, Wang X L, Fan F and Li W 2013 *Acta Phys. Sin.* **62** 130702 (in Chinese)
[11] Piccirillo C, Binions R and Parkin I P 2007 *Chem. Vapor Depos.* **13** 145
[12] Kana Kana J B, Ndjaka J M, Vignaud G, Gibaud A and Maaza M 2011 *Opt. Commun.* **284** 807
[13] Wang N, Magdassi S, Mandler D and Long Y 2013 *Thin Solid Films* **534** 594
[14] Nagashima K, Yanagida T, Tanaka H and Kawai T 2006 *Phys. Rev. B* **74** 172106
[15] Sun D D, Chen Z, Wen Q Y, Qiu D H, Lai W E, Dong K, Zhao B H and Zhang H W 2013 *Acta Phys. Sin.* **62** 017202 (in Chinese)
[16] Yoon M H and Seongil I 2005 *Appl. Surf. Sci.* **244** 444
[17] Lee M H and Kim M G 1996 *Thin Solid Films* **286** 219
[18] Cho C R, Cho S, Vadim S, Jung R and Yoo I 2006 *Thin Solid Films* **495** 375
[19] Ferrara D W, Nag J, MacQuarrie E R, Kaye A B and Haglund R F Jr 2013 *Nano Lett.* **13** 4169
[20] Shin S, Suga S, Taniguch Mi, Fujisawa M, Kanzaki H, Fujimori A, Daimon H, Ueda Y, Kosuge K and Kachi S 1990 *Phys. Rev. B* **41** 4993
[21] Zhang H F, Wu Z M, Yang W Y and Jiang Y D 2013 *Vacuum* **94** 84
[22] Yin W, Wolf S, Ko C, Ramanathan S and Reinke P 2011 *J. Appl. Phys.* **109** 024311
[23] Xu G, Huang C M, Tazawa M, Jin P, Chen D M and Miao L 2008 *Appl. Phys. Lett.* **93** 61911
[24] Orlianges J C, Leroy J, Crunteanu A, Mayet R, Carles P and Champeaus C 2012 *Appl. Phys. Lett.* **101** 133102
[25] Tao Z, Han T R T, Mahani S D, Duxbary P M, Yuan F and Ruan C Y 2012 *Phys. Rev. Lett.* **109** 166406